Optical Materials 138 (2023) 113715

Contents lists available at ScienceDirect

Optical Materials

journal homepage: www.elsevier.com/locate/optmat

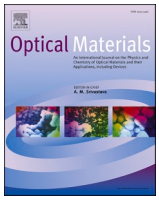

Field optimization for bifacial modules

Daniela Fontani [a,*], David Jafrancesco [a], Paola Sansoni [a], Andrea Nicolini [b], Alessia Di Giuseppe [b], Aron Pazzaglia [b], Beatrice Castellani [b], Federico Rossi [b], Luca Mercatelli [a]

[a] CNR-INO Largo E, Fermi 6, 50125, Firenze, Italy
[b] University of Perugia, CIRIAF, Via G.Duranti 67, 06125, Perugia, Italy

ARTICLE INFO

Keywords:
Bifacial PV
Retro-reflective (RR) materials
Ray tracing simulations
Field measurements

ABSTRACT

Bifacial modules are gaining more and more interest in PV market applications and strategies of major manufacturers. The bifacial photovoltaic module is able to generate energy from both sides of the photovoltaic cell, thus increasing the energy production compared to a standard photovoltaic module. In order to obtain the maximum production from a bifacial panel, all the characteristics that influence its performance must be studied and optimized. The specific aim of this research work is the design of a bifacial photovoltaic field optimized for the exploitation of the albedo of the soil. The study for minimizing losses due to light reflection on the ground was conducted considering the following aspects: identification of suitable materials, optical simulations of possible configurations, field measurements on a small-scale system. To improve the RetroReflectivity (RR) of the ground the optimal RR material is the one with a diameter of microspheres of 200–300 μm regardless of density. From the optical simulations the best configuration is a mixed ground with diffusive parts and a RR part. The results of the measurements show that once the ground is prepared in an appropriate way, we can have more than a 10% improvement in maximum power achieved and 2/3 of the light that hits the ground can be recovered.

1. Introduction

Bifacial modules are carving out an increasingly significant space within the photovoltaic market and the strategies of the main manufacturers. The bifacial photovoltaic module is a particular type of panel that manages to generate energy from both sides of the photovoltaic cell, thus increasing energy production compared to a standard photovoltaic module [1,2]. The increase in production that a bifacial module can guarantee, thanks to the capture of the light reflected from the ground on the rear side, is a much appreciated advantage in large ground-mounted plants, for which payback times are still the most important item today. For this reason, it is necessary to install components that can guarantee high production of electricity and better performance. This research work aims to achieve an efficiency of the photovoltaic system under standard conditions 25% higher than the single-side configuration. For this purpose, different approaches have been studied in parallel and will be compared. The most promising solutions will be defined and tested in a demonstrator field. The particular objective of this study is the design of a bifacial photovoltaic field optimized for the exploitation of the albedo of the soil. Albedo, i.e. the fraction of solar radiation reflected by a surface, is a well investigated characteristic of the ground that can affect the power output of the bifacial photovoltaic modules. Under this framework, the purpose is to identify suitable materials, to be deposited on the ground under and around the modules, in order to decrease the part of radiation that is not exploited by the modules, which would therefore be lost.

The objective of the first phase of this research was identifying suitable materials to be applied on the pavement on which a bifacial photovoltaic field is installed, in order to improve its energy production performance. To this aim, highly reflective and retro-reflective (RR) materials have been proposed thanks to their optical properties: highly reflective or diffusive materials typically follow the Lambert's cosine law, reflecting the incident radiation in all directions whilst RR materials reflect the incident radiation mainly towards the same direction of the incident one [3–7]. In Rossi et al., 2014 [3], an analytical model was introduced to describe the RR behavior in terms of angular distribution of the reflected radiation and a concentration factor "n" was introduced to indicate the amount of the radiation reflected by RR materials around the direction of incidence. According to that, "n" factor is unitary for diffusive materials and higher than 1 for RR materials due to their directional reflectivity properties [3].

RR materials are used for decades for traffic applications, i.e. in road

* Corresponding author.
E-mail address: daniela.fontani@ino.cnr.it (D. Fontani).

https://doi.org/10.1016/j.optmat.2023.113715
Received 27 December 2022; Received in revised form 2 March 2023; Accepted 19 March 2023
Available online 5 April 2023

traffic signs and reflectors to enhance the nighttime visibility. However, they have been largely investigated in literature, together with diffusive ones, as building coatings since they play a very important role on building energy balance and represent an innovative adaptation and mitigation measure to counterbalance Urban Heat Island (UHI) and Urban Heat Stress phenomenon thanks to their cooling effect [8–10].

RR coatings for building applications are typically made by glass beads laid on a reflecting substrate [6]. The potential benefits of diffusive and RR materials applied on urban context have been proved by several studies through their optical characterization (i) in-lab (i.e., through spectrophotometer equipped with an integrating sphere): in terms of global reflectance and angular distribution analysis (ii) in-situ (i.e., through pyranometer, spectro-radiometer); in a structure useful to represent a dense urban context (i.e., a small scale facility with a geometrical configuration of an urban canyon) [11]. In Gambelli et al., 2019 [12], an ad hoc experimental facility was introduced since the traditional in-lab and in-situ instruments could not completely describe the RR behavior due to their directional properties.

In Cardinali et al., 2022 [13], an in-situ experimental campaign was carried out in an inner courtyard, which consists of four facing walls, used to simulate an urban canyon in a small scale. Different canyon coating combinations of diffusive and RR materials and height/width (H/W) ratios were assessed in terms of albedo in the canyon facility. The results showed that the highest albedo value resulted equal to 4.7% for a canyon's H/W equal to 0.5 when the RR material was applied on walls coupled with diffusive coating on pavement.

In Morini et al., 2017 [14], concrete cubes were used to simulate urban structures with different geometry and orientations (i.e., blocks, W-E canyons and N–S canyons) in which RR films were applied on lateral surfaces (which represent building façades). Results showed an improvement in terms of equivalent albedo equal to 3% in block scheme and to 7% both in W-E and N–S canyon configurations.

In Rossi et al., 2015 [15], an experimental study was made by two twin arrays which simulate small size urban canyons with different H/W ratio and façades coatings (RR or diffusive materials). Results showed that RR coatings allow 1–2% reduction of the energy trapped into the canyon.

Starting from the state of the art in the literature, this study investigates the effect of diffusive and RR materials applied as ground envelopes of the bifacial photovoltaic field with the aim of extending their range of application, thanks to their optical properties.

In the literature there are articles with tests performed on photovoltaic solar fields that consider soils with grass and standard materials (white paint [16] or concrete [17]) or discuss tests on roofs always using standard materials (Medium Brown Shingles, White Tiocoat/Swarco Beads, Aluminum Paint [18]).

To the best of our knowledge, there are no other studies in the literature on such solutions for improving bifacial photovoltaic performance.

The study was conducted considering the following aspects: identification of suitable materials for the maximization of the light reflected from the ground to the back side of the panel, optical simulations of the possible configurations considering the different materials on the ground, field measurements on a small scale system utilizing the selected materials and the chosen configuration.

2. Materials for albedo optimization

The present research represents a final effort in the investigation of the optimum design of RR coatings to be used in combination with diffusive materials on the ground of a bifacial photovoltaic field. The aim is to optimize the collected solar radiation and so to increase the electric energy produced by the downward photovoltaic modules. Under this framework, previous works have been carried out by varying the substrate materials and roughness, the glass beads density and dimension ranges of RR material samples [19,20], which are the key parameters affecting their performances.

Firstly, in a previous work [19] three types of substrate materials characterized by different roughness, have been investigated to evaluate their effect on the optical performance of RR coatings. Results showed that the roughest RR material made by a plywood panel provided the highest RR capability, equal to 16%, with respect to the other samples characterized by a homogeneous and smooth surface [19]. RR material made by a plywood panel resulted the best performing RR sample also after outdoor aging and soiling in summer. Secondly [20], several RR materials have been realised with different diameter and superficial density ranges of RR glass beads in order to further explored the optimum design of RR materials. Five diameter ranges (i.e., $\varphi_1 = 40 \div 70$ μm, $\varphi_2 = 70 \div 110$ μm, $\varphi_3 = 100 \div 200$ μm, $\varphi_4 = 200 \div 300$ μm and $\varphi_5 = 400 \div 800$ μm) and three superficial density ranges of glass beads (i.e., $\rho_{s1} = 0.30 \div 0.40$ kg/m^2, $\rho_{s2} = 0.20 \div 0.30$ kg/m^2 and $\rho_{s3} = 0.10 \div 0.20$ kg/m^2) have been investigated. The optical performance of RR materials has been tested in lab through spectrophotometric and angular reflection distribution analysis. Results showed that RR materials with 200 ÷ 300 μm diameter exhibited the highest RR capability, both in terms of Global Reflectance (GR) and angular distribution analysis around the incident direction, regardless of the superficial density [20].

Starting from the previous results [19,20], a plywood panel and glass beads with an average diameter of 200 ÷ 300 μm (φ_4) and superficial density range equal to 0.20 ÷ 0.30 kg/m^2 (ρ_{s2}) have been selected to realize four RR material samples in this study. As reported in Cardinali et al., 2022 [20], $RR_{\varphi4,\ \rho s2}$ provided a GR equal to 75.6% [20]. In Fig. 1, the angular reflectivity distribution of $RR_{\varphi4,\ \rho s2}$ is presented for an incident radiation angle of −20° and −30° with respect to the normal incident direction. These distributions were obtained by the measurement facility and methods already described in Ref. [20].

RR component [%] is calculated as the percentage of back-reflection, over the sum of the reflections measured for $RR_{\varphi4,\ \rho s2}$ in all the investigated directions. RR component resulted equal to 16.1% at −20° and 16.0% at −30° of incident direction for $RR_{\varphi4,\ \rho s2}$ [20].

The RR coating samples were made by a highly reflective white paint, supplied by INDEX Construction Systems and Products S.p.A. [21], on which RR glass beads with an average diameter of 200 ÷ 300 μm, supplied by Prochima® S.r.l. [22], were manually dispersing as homogeneous as possible on the top. Also, diffusive samples made by the same highly reflective white paint without glass beads on the top were realised. Fig. 2 shows the investigated RR samples. The size of the substrate materials was 27 cm × 54 cm.

3. Field optical simulations

A solar field with photovoltaic panels is presented in Fig. 3. The photo shows the solar field before the modifications that will be implemented on the field in the final phase of the research work. The solar field consists in several photovoltaic panels without sun tracking, oriented towards the South direction and tilted of 57 deg with respect to the horizontal plane. This tilt angle represents the best solution at the installation latitude in order to maximise the solar energy collection by the panels.

A section of the solar field with PV panels was simulated by means of a non-sequential optical simulation software (TracePro, Lambda Research Corp.).

Optical CAD tools fall into two categories: sequential software, when the user must set the order in which the rays impinge the system surfaces, and non-sequential software, when every optical ray, emitted by the source according to its geometrical emittance properties, hits the first surface found on its path and then the others according to reflectance and refractive laws (it simulates better the physical reality). The sequential software permits to calculate the aberration values and the characteristics of the wavefront, while the non-sequential ones are specialized in the evaluation of the radiometric and photometric quantities. In particular, among these outputs of the non-sequential software,

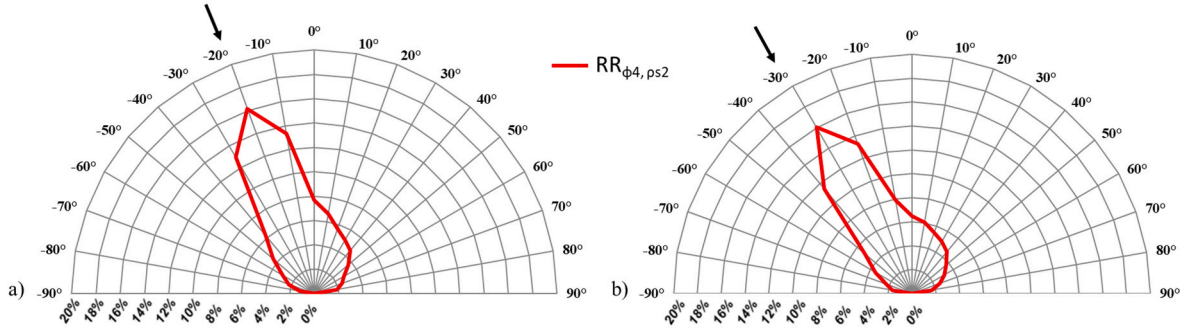

Fig. 1. Angular reflection distribution of the RR material with 200 ÷ 300 μm of glass beads size and 0.20 ÷ 0.30 kg/m^2 of beads' superficial density for an incident radiation angle of −20° (a) and −30°(b) [15].

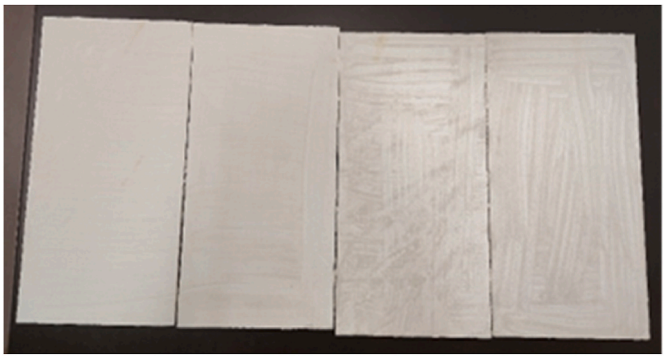

Fig. 2. Investigated RR samples made by plywood panels with 200 ÷ 300 μm of glass beads size and 0.20 ÷ 0.30 kg/m^2 of beads' superficial density.

Fig. 3. Solar field with PV panels. Actual distances and heights are transferred in a simulation software.

very useful data for our applications are the irradiance maps, that show the distribution of the light on a surface.

The section of the field is composed of six PV panels distributed in two rows of three panels each. The simulation calculates the radiation that, impinging on a certain section of the ground, is reflected toward the PV panels around it. For this reason, actual distances and heights (Fig. 3) are calculated from the real solar field and transferred in the simulation software.

In the simulation procedure the part of the ground considered is the one behind the central solar panel (Fig. 4), in the matrix position (0,0). The simulation is aimed to determine the part of the radiation reflected by the ground and impinging on each of the six PV panels. In the TracePro simulation the detectors are represented by the front and rear

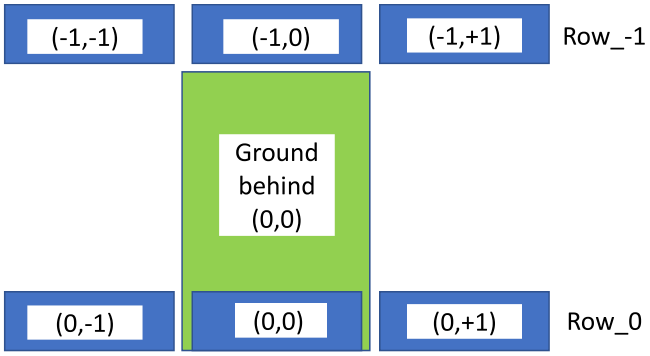

Fig. 4. Positions of the components on the simulated field (schematic view from above). The (0,0) PV panel is the reference one.

surfaces of the PV panels. The PV panels are set as total absorbers.

In Fig. 5 Lambertian material and retroreflective material are compared.

The reflective characteristics of the ground considered are three: Lambertian diffuser (80% reflection), retroreflective material (data from Sect.2 "Materials for albedo optimization"), and a mixture of the two types (part of the ground with diffusing properties and part with retroreflective properties). The retroreflective sheet was simulated as an opaque surface with the following properties: absorbance 15%, specular reflection 15%, diffuse reflection 85%; the radiation lobe of the diffuse reflection was set by means of a Bi-directional Reflectance Distribution Function (BRDF), defined using an ABg model (A = 0.13064, B = 0.08, g = 1.5) [23].

The mixed solution (Fig. 6) was proposed due to the characteristics of the retroreflective material: since it reflects the large part of the radiation back, close to the direction of the impinging light, then the RR material is useful when it is hit by radiation that passes nearby the panel edge.

We stress that only for the surface near the PV panel there is an advantage from the utilization of the retroreflective material, while for the surface far from the PV panel is better to have a Lambertian reflection. In order to roughly evaluate where the RR material has to be placed, a comparison between the angular distribution of the light reflected by the RR material and a Lambertian surface was made. It shows that the light intensity reflected by the RR material is of the same order than the intensity reflected by the Lambertian surface when the angle between incident and reflection directions is about 30 deg. Then, due to the fact that.

- the distance between the panels is 7.1 m (see Fig. 3);
- the height of the panel is 2.96 m (see Fig. 3) and its tilt is 57 deg;

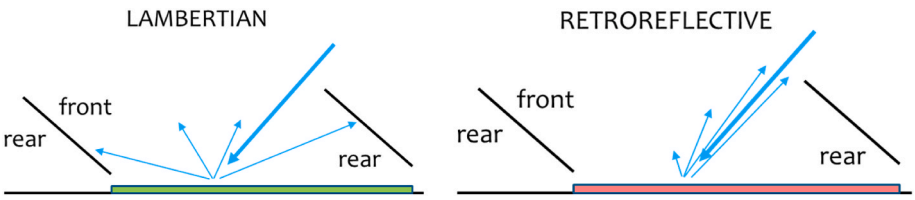

Fig. 5. Ground with different materials: Lambertian material (left); retroreflective material (right).

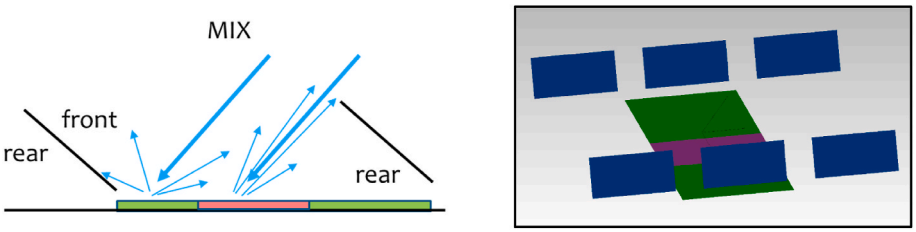

Fig. 6. The proposed mixed solution. Lateral view (left) and 3D view (right). The ground in green color is made of Lambertian material, while the ground in pink color is made of RR material.

- in Italy, the maximum sun elevation angle is about 75 deg;

it is possible to estimate that the zone where the RR material should have a better performance with respect to the Lambertian one is comprised between the edge of the Row_0 (projected on the ground) and a line 2.96 m from the edge of the Row_0.

In practice, due to the fact that in Italy the sun elevation does not exceed 75 deg, the RR material should cover only a strip on the ground located between a line about 0.79 m from the edge of the Row_0 and the line 2.96 m from the edge of the Row_0.

The radiation reflected by the portion of the ground considered impinges mainly on the rear of the PV panels of Row_0 and on the front and rear of the panels of Row_-1, indeed, as the panels of Row_-1 are suspended with respect to the ground, the reflected radiation impinges both on front and rear.

In the simulation the position of the sun is fixed and set perpendicular to the PV panels, in an optimized configuration, as to improve the differences between each case.

In this configuration the direct solar radiation on panel (0,0) is equal to 23760W, while the radiation impinging on the ground considered is 56356W. In the case of ground Lambertian diffuser the total amount of radiation reflected is 6530W and the ratio reflected/direct radiation is 27.4%. This means that an amount equal to the 27.4% of the radiation which impinges on solar panel (0,0) is reflected from the ground and hits the back or front surface of one of the PV panels.

In the case of retroreflective ground, the total radiation reflected is 6755W, 28.4% of the direct radiation.

In the mixed solution, the retroreflective material is deposed in a stripe 10.57 m $\times$ 2.25 m (width x deep); its center is about 1.87 m from the projection on the ground of the upper edge of the first row of mirrors.

In this arrangement, the radiation recovered by the ground behind central panel is the 29.6% of the one which impinges on the panel itself. The sun is simulated as a grid source placed above the panels, which uniformly emits rays with the correct solar divergence (total angle = 0.54 deg).

The results obtained from the TracePro simulation with 6384000 starting rays are reported in Table 1 for the three ground surfaces examined: Lambertian, Retroreflective and Mixed solution.

The result shows clearly that the mix of Lambertian and retroreflective material offers the best solution in order to collect the maximum quantity of radiant flux.

Table 1
Simulation results.

	LAMBERTIAN	RETROREFLECTIVE	MIXED SOLUTION
Direct Flux on the panel (W)	23760	23760	23760
Flux on the ground (W)	56356	56356	56356
Total flux reflected (W)	6530	6755	7036
Reflected flux/Direct flux (%)	**27.4**	**28.4**	**29.6**

4. Outdoor tests

ENEL, coordinator of the project *Best4U*, supplied 5 double-sided minimodules to carry out the outdoor tests. Each minimodule has square shape, with lateral dimension 36 cm.

The mini-modules are characterized by having 4 photovoltaic cells on both sides of the PV panel. The Front side is the one directly exposed to solar radiation, while the Back side receives diffused radiation from the ground. Two measurement campaigns were carried out for the outdoor tests.

During each measurement campaign the values acquired were.

- total irradiance with Pyranometer and direct irradiance with Pyrheliometer mounted on the sun tracker supplied by INO;
- 3 sampling cycles of the VI curve (Voltage Current curve) using the Rigol DL3021A variable load;
- Voc (Open Circuit Voltage) before the measurement;
- ambient temperature before and after the measurement;
- temperature of the mini-modules cells for both panel sides before and after the measurement.

For a comparison with the use of traditional photovoltaic cells (single face) the measurements were of two types.

- Front measurement, performed on the Front of the mini-module, obscuring the Back part of the minimodule:
- Front + Back measurement, performed on the Front and on the Back of the minimodule, using the minimodule entirely with both sides exposed to the radiation.

In the first campaign, which was meant to serve as a reference, the arrangement of the minimodules was not aimed at maximising the

contribution of the diffused light. Instead for the second measurement campaign the configuration resulting from the simulations with the optimization of the real field was reproduced in scaled form.

In the second test campaign the minimodule was surrounded by diffusive plywood panels, tinted with a high reflecting paint, as Fig. 7 shows. The orientation of the minimodule is daily adjusted in order to have the radiation at noon impinging perpendicularly to the minimodule surface, considering the local latitude and the day of the year. Moreover, in the part of the ground facing the rear side of the minimodule alternately was posed one of the 4 RR panels or 1 diffusive panel, this one always realised with the reflective paint. To complete the measurements, the last measurement of the set is performed without plywood panels and with a black background, as reference. This last measurement was usually taken around the 1:00 p.m. (solar time), so the inclination of the solar rays is still quite perpendicular to the minimodule surface.

5. Results and discussion

Fig. 8 and 9 present the graphs obtained in the same day but in different moments of the daytime: Fig. 8 is taken during the morning, while Fig. 9 around the local noon, where is expected the peak on the PV modules, since the radiation impinges normally to the minimodule surface. Considering that noon is the time in which the simulation was made, it is expected that the effects of the RR materials reach the maximum of the contribution. The morning measurement serves to verify if this contribution is still effective at a time other than noon.

Each graph reports only the results of the Front + Back measurements for several configurations because the Front measurements do not show a difference between the various configurations. The configurations are indicated in the legends specifying the type of panel, RR plywood panel (nr1, …, nr4) or diffusive panel (diffuser), and the mean value of total irradiance (W/m2). In addition, in Fig. 8 there is a reference measurement ("old" in the legend) made in the first test campaign. The measurements of the first test campaign were taken with no adaptation of the ground, which is on composed of grey stone, as it is visible in Fig. 7. The measurement labelled as "old" was chosen because its total irradiance was the nearest to the average irradiance values measured in the morning.

In Fig. 9 the reference measurement is the last one of the daily measurements, made with the black background ("black" in the legend).

The effectiveness of using a configuration with a ground optimized for light diffusion is evident in the comparison among the Front + Back measurements with each reference measurement ("old" in Fig. 8 or "black" in Fig. 9).

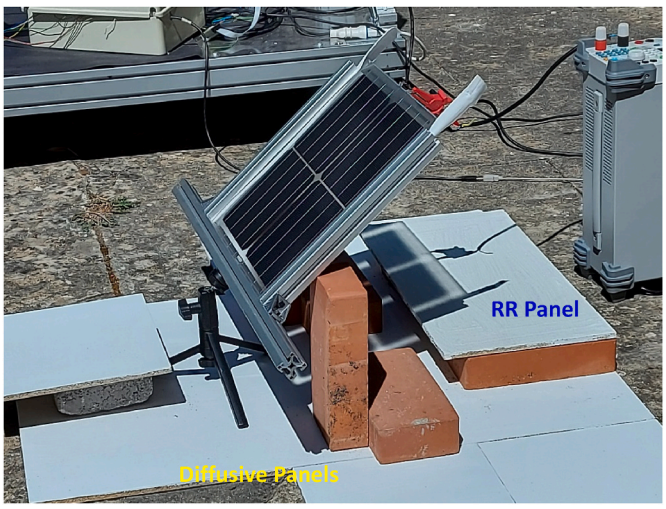

Fig. 7. Measurement set-up for the outdoor tests of the minimodule in the second test campaign.

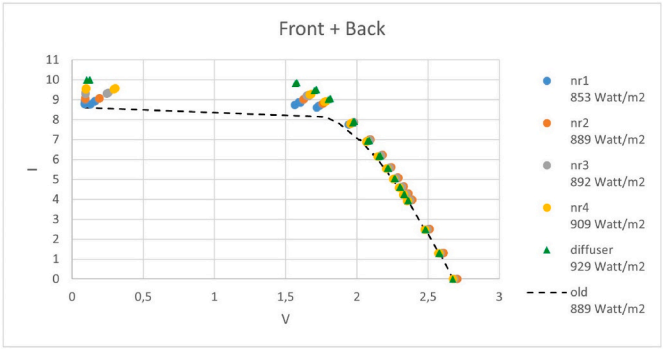

Fig. 8. Morning measurements on Front and Back of the minimodule for the configurations indicated by the type of panel, RR plywood panel (nr1, …, nr4) or diffusive panel (diffuser), and the mean value of total irradiance (W/m2).

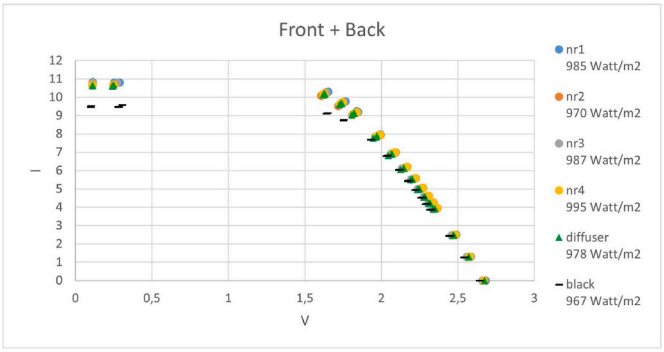

Fig. 9. Measurements taken around the local noon on Front and Back of the minimodule for the configurations with RR plywood panel (nr1, …, nr4) or diffusive panel (diffuser), and the written mean value of total irradiance (W/m2).

Tables 2 and 3 show the values of the short-circuit current (Isc), the open circuit voltage (Voc) and the maximum of power (Pmax). The value of Voc has been measured, while the values of Isc and Pmax have been calculated interpolating the measured data. Table 2 corresponds to Fig. 2, while Table 3 reports the values for Fig. 3. The maximum value of each column is evidenced in red. The last column of each table reports (ΔPmax in percentage) the difference between the power of each configuration and the reference power. The reference is evidenced in violet on the table. In Tables 2 and 3 there is a line that presents the average of the measurements performed on RR plywood panel because the production of these panels has not been already optimizes, so the tables data show variations among the different samples.

To verify the effectiveness of the experimented configurations, the results of the Front + Back measurements have been compared with the results of the Front measurements.

Table 2
Morning measurements on Front and Back of the minimodule for the configurations indicated by the type of panel.

Front + Back (morning)				
Configuration	Isc	Voc	Pmax	ΔPmax (%)
N1	8,95	2,70	15,35	4,98%
N2	9,09	2,70	15,81	8,15%
N3	9,36	2,68	15,94	9,04%
N4	9,60	2,67	15,84	8,36%
Mean N1–N4	*9,25*	*2,69*	*15,74*	*7,63%*
Diffuser	10,02	2,67	16,35	11,86%
Old	8,63	2,67	14,62	

Table 3
Measurements taken around the local noon on Front and Back of the minimodule for the configurations.

Front + Back (noon)				
Configuration	Isc	Voc	Pmax	ΔPmax (%)
N1	10,86	2,68	17,16	11,82%
N2	10,74	2,67	16,71	8,89%
N3	10,92	2,66	16,84	9,72%
N4	10,76	2,67	16,75	9,16%
Mean N1–N4	*10,82*	*2,67*	*16,87*	*9,90%*
Diffuser	10,71	2,67	16,7	9,08%
Black	9,70	2,64	15,35	

For the measurements performed at noon, Table 4 reports the maximum power calculated for the Front and Front + Back measurements.

The increment of the power (in column 4 of Table 4) obtained in the Front + Back measurements has been calculated referring to the power value of the Front measurement for the "black" configuration. Considering that the power obtained in the Front measurement is almost constant (in column 2 of Table 4), this confirms that there is no significant difference between the various configurations, and the Pmax for the reference configuration is comparable with the others. The situation is completely different for the Front + Back measurement that shows an increment of 4,30% for the black panel. Moreover, the Pmax values of Front + Back for the configuration with an optimized ground can reach a maximum improvement of 16,63% using panel N1, but the increment is greater than 10% for all configurations, included the diffuser panel.

The results for the RR panels show some variability due to the fact that the production process is not yet standard.

From the raytracing simulations the amount of recovered flux for the panel 0,0 was 4220W in case of diffusive ground and 4845W in case of mixed ground. Since the raytracing simulations do not take into account the angular response of the PV panel, the value of reflected flux calculated on the simulations represents a maximum amount for the electrical power output. A reasonable minimum for the electrical power output could be the half of the calculated value. This means that the expected ΔPmax, calculated as the ratio between the recovered power of each configuration and the Direct Flux on the panel, in Table 1 for the diffusive case was expected between 17.7% and 8,8%, and for the mixed case was expected between 20.3% and 10.1%.

The results are both in the expected range and show that at least of 2/3 of the flux that impinges on the back side of the minimodule is converted in electrical power.

6. Conclusions

This research work studies fields of solar collection with bifacial photovoltaic (PV) cells, trying to obtain an efficiency for a solar field of bifacial cells higher than 25% compared to the standard configuration, with only one side of the PV module with cells.

The purpose of this work is to find materials and field configuration to optimize the efficiency of the bifacial photovoltaic minimodules through the optimization of the solar field. This article presents an innovative approach trying to maximise the collected sun power for the back side of a bifacial PV module, performing a study on suitable materials and ray tracing simulations.

In this work some suitable Retro-Reflective (RR) materials have been studied and realised to minimise the flux lost because it does not reach the rear part of the panel and maximise the recovery of the solar flux. The study analyses the optical properties of a set of RR materials characterized by different distribution density and diameter of glass microspheres. As the diameter of the microspheres (d in μm) increases, at the same density, the performance in terms of RR behaviour improves, with a maximum value of RR component for d = 200–300 μm for all angles of incidence. As the density (kg/m^2) increases, with the same diameter of microspheres, the performance in terms of RR behaviour generally improves. Thus, by taking into account also the measurement results of global spectral reflectance, it was found that the optimal RR material is the one with a diameter of microspheres of 200–300 μm regardless of density.

For the field optimization a ray tracing analysis was performed in order to obtain the best configuration considering a real field and the materials examined in the previous study, both diffusive and RR. As result of these simulations the best configuration is a mixed ground with diffusive parts and a RR part. The RR part is located in an area behind the photovoltaic panel.

Some tests on a scaled field with a single minimodule was performed in order to verify the effectiveness of the optimisations combining the results of the material studies and raytracing simulations. The measurement was executed in the summer season, 2 sets of measurements were performed on the same PV module alternating the 4 RR panels realised and the diffusive one. Moreover, a measure with a black panel in a grey ground was done as reference for the noon measurement. The comparison between the measurements performed with and without the plywood panels on the ground shows that there is an improvement of the minimodule output when the ground is properly settled.

RR materials are most effective when the sun's position reaches noon, which is the time in which the field has been optimized. The results show that the realisation of an optimized field could improve the maximum power of the module at noon more than 10% with respect to the traditional PV module, with PV cell only on the front side.

Table 4
Comparison of the Front measurements with the Front + Back measurements at noon for the configurations.

Front/Front + Back (noon)			
Configuration	Front Pmax	Front + Back Pmax	ΔPmax (%)
N1	14,63	17,16	16,63%
N2	14,73	16,71	13,57%
N3	14,56	16,84	14,44%
N4	14,44	16,75	13,85%
Mean N1–N4	*14,59*	*16,87*	*14,62%*
Diffuser	14,37	16,74	13,77%
Black	14,71	15,35	4,30%

CRediT author statement

D. Fontani: Conceptualization, Data curation, Investigation, Validation, Writing - original draft;

D. Jafrancesco: Data curation, Investigation, Validation, Writing - original draft;

P. Sansoni: Investigation, Writing - original draft; Writing - review & editing;

A. Nicolini: Conceptualization, Methodology, Validation, Writing - review & editing;

A. Di Giuseppe: Investigation, Writing - original draft;

A. Pazzaglia: Investigation, Writing - original draft;

B. Castellani: Conceptualization, Methodology, Validation, Writing - review & editing;

F. Rossi: Supervision, Writing - review & editing;

L. Mercatelli: Conceptualization, Writing - review & editing, Project administration; Funding acquisition.

Declaration of competing interest

The authors declare that they have no known competing financial interests or personal relationships that could have appeared to influence the work reported in this paper.

Data availability

I have shared my data in the ANNEX1 section

Acknowledgements

The present experimental research was funded by the MInistero dell'Universita e della Ricerca (MUR) Italian Ministry of University and Research (MUR) under the PON Project entitled "BEST4U-Bifacial Efficient Solar Cell Technology with 4-Terminal Architecture for Utility Scale".

ANNEX1.

Table A.1
Data for Fig. 8

panel name/direct power mean											
nr1 853 Watt/m2		nr2 889 Watt/m2		nr3 892 Watt/m2		nr4 909 Watt/m2		Diffuser 929 Watt/m2		Old 889 Watt/m2	
V	I	V	I	V	I	V	I	V	I	V	I
2,70	0,00	2,70	0,00	2,68	0,00	2,67	0,00	2,67	0,00	2,68	0,00
2,60	1,30	2,61	1,31	2,59	1,29	2,57	1,29	2,58	1,29	2,59	1,27
2,50	2,50	2,51	2,51	2,49	2,50	2,48	2,48	2,48	2,48	2,58	1,27
2,37	3,96	2,39	3,98	2,37	3,96	2,35	3,92	2,36	3,93	2,58	1,27
2,34	4,27	2,36	4,30	2,35	4,27	2,33	4,24	2,33	4,25	2,49	2,40
2,31	4,62	2,33	4,65	2,31	4,62	2,29	4,59	2,30	4,60	2,49	2,40
2,27	5,04	2,29	5,09	2,27	5,07	2,26	5,01	2,26	5,04	2,48	2,39
2,22	5,55	2,24	5,61	2,23	5,59	2,21	5,54	2,21	5,55	2,38	3,73
2,15	6,16	2,17	6,22	2,17	6,18	2,14	6,14	2,15	6,16	2,37	3,72
2,07	6,89	2,09	6,99	2,09	6,96	2,07	6,89	2,07	6,93	2,37	3,71
1,94	7,76	1,97	7,86	1,97	7,86	1,95	7,78	1,97	7,85	2,35	3,99
1,72	8,60	1,76	8,81	1,78	8,90	1,77	8,89	1,80	9,02	2,35	3,99
1,56	8,74	1,63	9,02	1,65	9,20	1,67	9,26	1,70	9,47	2,34	3,99
0,13	8,77	0,19	9,05	0,24	9,30	0,29	9,53	1,57	9,82	2,32	4,31
0,09	8,79	0,09	9,05	0,09	9,30	0,10	9,52	0,12	9,98	2,32	4,30
0,09	8,79	0,09	9,08	0,09	9,31	0,10	9,53	0,10	9,98	2,31	4,29
2,60	1,30	2,61	1,31	2,59	1,30	2,57	1,29	2,58	1,29	2,29	4,69
2,50	2,50	2,51	2,51	2,49	2,49	2,48	2,48	2,48	2,48	2,28	4,68
2,37	3,96	2,39	3,98	2,37	3,96	2,35	3,93	2,36	3,93	2,28	4,68
2,34	4,27	2,36	4,30	2,35	4,27	2,33	4,24	2,33	4,24	2,24	5,13
2,31	4,62	2,33	4,65	2,32	4,62	2,30	4,59	2,30	4,61	2,24	5,12
2,27	5,05	2,29	5,10	2,28	5,07	2,26	5,03	2,26	5,04	2,24	5,11
2,22	5,56	2,24	5,61	2,23	5,59	2,21	5,54	2,22	5,55	2,19	5,64
2,16	6,17	2,18	6,22	2,17	6,20	2,15	6,15	2,16	6,17	2,18	5,61
2,07	6,93	2,09	7,00	2,09	6,96	2,07	6,90	2,08	6,95	2,18	5,63
1,95	7,78	1,98	7,87	1,98	7,87	1,96	7,83	1,98	7,90	2,12	6,28
1,73	8,69	1,77	8,83	1,78	8,91	1,78	8,90	1,81	9,04	2,11	6,24
1,60	8,85	1,63	9,03	1,67	9,18	1,68	9,27	1,71	9,50	2,11	6,24
0,16	8,92	0,19	9,07	0,25	9,31	0,30	9,55	1,58	9,85	2,02	7,00
0,09	8,89	0,09	9,07	0,09	9,30	0,10	9,56	0,12	9,99	2,02	6,99
0,09	8,90	0,09	9,07	0,10	9,31	0,10	9,57	0,10	9,99	2,02	6,99
2,60	1,30	2,61	1,31	2,59	1,30	2,58	1,29	2,58	1,29	1,87	7,85
2,50	2,50	2,51	2,51	2,49	2,50	2,48	2,48	2,48	2,49	1,86	7,84
2,37	3,96	2,39	3,98	2,37	3,96	2,36	3,93	2,36	3,94	1,86	7,84
2,34	4,27	2,36	4,30	2,35	4,27	2,33	4,24	2,34	4,26	1,78	8,14
2,31	4,62	2,33	4,65	2,32	4,63	2,30	4,59	2,31	4,61	1,78	8,13
2,27	5,05	2,29	5,09	2,28	5,07	2,26	5,03	2,27	5,04	1,78	8,13
2,22	5,56	2,24	5,61	2,23	5,59	2,21	5,55	2,22	5,56	0,09	8,60
2,16	6,17	2,18	6,23	2,17	6,20	2,15	6,15	2,16	6,20	0,09	8,59
2,07	6,93	2,10	7,01	2,09	6,96	2,07	6,93	2,09	6,96	0,09	8,58
1,96	7,78	1,98	7,87	1,98	7,87	1,96	7,84	1,98	7,92	0,09	8,58
1,74	8,70	1,77	8,82	1,78	8,92	1,78	8,92	1,82	9,06	0,09	8,59
1,59	8,87	1,63	9,02	1,66	9,23	1,68	9,29	1,72	9,51	0,09	8,58
0,16	8,93	0,19	9,07	0,26	9,35	0,31	9,58	1,58	9,86	0,09	8,57
0,09	8,93	0,09	9,03	0,10	9,35	0,10	9,57	0,13	10,00	0,09	8,56
0,09	8,93	0,09	9,03	0,10	9,34	0,10	9,58	0,10	10,00	0,09	8,55

Table A.2
Data for Fig. 9

panel name/direct power mean											
nr1 985 Watt/m2		nr2 970 Watt/m2		nr3 987 Watt/m2		nr4 995 Watt/m2		Diffuser 978 Watt/m2		Black 967 Watt/m2	
V	I	V	I	V	I	V	I	V	I	V	I

(*continued on next page*)

Table A.2 (*continued*)

panel name/direct power mean											
nr1 985 Watt/m2		nr2 970 Watt/m2		nr3 987 Watt/m2		nr4 995 Watt/m2		Diffuser 978 Watt/m2		Black 967 Watt/m2	
V	I	V	I	V	I	V	I	V	I	V	I
2,68	0,00	2,67	0,00	2,66	0,00	2,67	0,00	2,67	0,00	2,64	0,00
2,58	1,30	2,57	1,29	2,56	1,28	2,57	1,29	2,57	1,29	2,54	1,27
2,49	2,49	2,47	2,47	2,46	2,46	2,48	2,48	2,47	2,48	2,44	2,44
2,37	3,95	2,35	3,91	2,34	3,89	2,36	3,93	2,35	3,93	2,32	3,86
2,34	4,26	2,32	4,23	2,31	4,21	2,33	4,25	2,32	4,23	2,29	4,17
2,31	4,62	2,29	4,58	2,28	4,55	2,30	4,60	2,28	4,55	2,26	4,52
2,27	5,05	2,25	5,00	2,24	4,99	2,26	5,04	2,23	4,97	2,22	4,93
2,23	5,58	2,20	5,53	2,19	5,50	2,22	5,55	2,19	5,50	2,17	5,43
2,17	6,20	2,15	6,12	2,14	6,10	2,16	6,16	2,13	6,06	2,11	6,04
2,09	7,00	2,07	6,92	2,06	6,87	2,08	6,94	2,04	6,82	2,03	6,79
1,99	7,98	1,97	7,85	1,96	7,82	1,97	7,84	1,95	7,76	1,93	7,68
1,84	9,23	1,81	9,05	1,81	9,04	1,81	9,05	1,81	9,03	1,75	8,78
1,76	9,77	1,72	9,51	1,73	9,60	1,73	9,60	1,73	9,60	1,65	9,14
1,65	10,29	1,61	10,08	1,62	10,13	1,62	10,11	1,62	10,12	0,31	9,59
0,28	10,80	0,26	10,69	0,27	10,78	0,25	10,65	0,24	10,62	0,10	9,53
0,11	10,81	0,11	10,69	0,11	10,79	0,11	10,65	0,11	10,63	0,10	9,53
2,59	1,29	2,57	1,29	2,57	1,29	2,58	1,29	2,57	1,29	2,55	1,28
2,49	2,49	2,48	2,48	2,47	2,47	2,48	2,48	2,47	2,47	2,45	2,45
2,37	3,95	2,35	3,93	2,35	3,91	2,36	3,93	2,34	3,91	2,32	3,87
2,34	4,26	2,33	4,24	2,32	4,23	2,33	4,24	2,31	4,21	2,30	4,18
2,31	4,61	2,30	4,59	2,29	4,58	2,30	4,61	2,28	4,56	2,27	4,53
2,27	5,06	2,26	5,03	2,25	5,00	2,27	5,04	2,24	4,99	2,23	4,96
2,22	5,58	2,22	5,55	2,21	5,54	2,22	5,58	2,20	5,53	2,18	5,46
2,17	6,20	2,16	6,16	2,15	6,15	2,17	6,18	2,15	6,12	2,12	6,06
2,09	7,00	2,08	6,95	2,08	6,94	2,09	6,99	2,07	6,92	2,04	6,80
1,99	7,98	1,98	7,91	1,98	7,91	1,99	7,94	1,97	7,84	1,93	7,68
1,85	9,19	1,83	9,14	1,83	9,15	1,84	9,17	1,82	9,12	1,75	8,73
1,76	9,75	1,74	9,63	1,74	9,71	1,75	9,72	1,74	9,64	1,64	9,11
1,64	10,27	1,63	10,13	1,63	10,23	1,62	10,20	1,63	10,15	0,29	9,49
0,29	10,80	0,25	10,65	0,27	10,79	0,25	10,66	0,24	10,63	0,10	9,48
0,11	10,81	0,11	10,65	0,11	10,78	0,11	10,66	0,11	10,64	0,10	9,48
2,58	1,29	2,58	1,29	2,58	1,29	2,58	1,29	2,57	1,29	2,55	1,28
2,48	2,49	2,48	2,48	2,48	2,48	2,48	2,49	2,47	2,47	2,45	2,45
2,36	3,94	2,36	3,93	2,36	3,93	2,37	3,95	2,34	3,89	2,33	3,87
2,33	4,25	2,33	4,24	2,33	4,25	2,34	4,26	2,31	4,21	2,30	4,19
2,30	4,61	2,30	4,61	2,30	4,60	2,31	4,61	2,28	4,56	2,27	4,53
2,27	5,04	2,26	5,04	2,26	5,04	2,27	5,05	2,25	5,00	2,23	4,96
2,22	5,58	2,22	5,55	2,22	5,55	2,22	5,58	2,20	5,53	2,18	5,46
2,17	6,20	2,16	6,17	2,16	6,16	2,17	6,20	2,15	6,14	2,12	6,06
2,09	7,00	2,09	6,96	2,09	6,96	2,09	6,99	2,07	6,89	2,04	6,81
2,00	7,94	1,99	7,93	1,99	7,93	1,99	7,92	1,97	7,89	1,93	7,69
1,84	9,23	1,83	9,16	1,84	9,17	1,83	9,14	1,82	9,13	1,75	8,73
1,76	9,75	1,74	9,70	1,75	9,74	1,74	9,64	1,74	9,70	1,64	9,11
1,65	10,27	1,63	10,16	1,64	10,25	1,63	10,14	1,63	10,21	0,28	9,47
0,25	10,81	0,24	10,64	0,26	10,75	0,25	10,66	0,25	10,66	0,10	9,48
0,11	10,82	0,11	10,64	0,11	10,76	0,11	10,66	0,11	10,67	0,10	9,47

References

[1] R. Kopecek, J. Libal, Bifacial photovoltaics 2021: status, opportunities and challenges, Energies 14 (2021) 2076, https://doi.org/10.3390/en14082076.

[2] R. Guerrero-Lemus, R. Vega, Taehyeon Kim, Amy Kimm, L.E. Shephard, Bifacial solar photovoltaics – a technology review, Renew. Sustain. Energy Rev. 60 (2016) 1533–1549, https://doi.org/10.1016/j.rser.2016.03.041.

[3] F. Rossi, A.L. Pisello, A. Nicolini, M. Filipponi, M. Palombo, Analysis of retroreflective surfaces for urban heat island mitigation: a new analytical model, Appl. Energy 114 (2014) 621–631, https://doi.org/10.1016/j.apenergy.2013.10.038.

[4] B. Castellani, A. Presciutti, E. Morini, E. Anderini, M. Filipponi, A. Nicolini, F. Rossi, in: Investigation on the Optic-Energy Interaction between Retro Reflective Façades and Pavement in Urban Canyons, Proceeding from the 4th International Conference on Countermeasures to Urban Heat Island (IC2UHI 2016), Singapore, 30 May–1 June 2016.

[5] J. Yuan, K. Emura, C. Farnham, Potential for Application of Retroreflective Materials Instead of Highly Reflective Materials for Urban Heat Island Mitigation, Urban Studies Research, 2016, 3626294, https://doi.org/10.1155/2016/3626294.

[6] J. Yuan, K. Emura, H. Sakai, C. Farnham, S. Lu, Optical analysis of glass bead retro-reflective materials for urban heat island mitigation, Sol. Energy 132 (2016) 203–213, https://doi.org/10.1016/j.solener.2016.03.011.

[7] B. Castellani, A. Nicolini, A.M. Gambelli, M. Filipponi, E. Morini, F. Rossi, Experimental assessment of the combined effect of retroreflective façades and pavement in urban canyon, in: Proceedings from the 10th International Conference IAQVEC 2019: Indoor Air Quality, Ventilation and Energy Conservation in Buildings, 5–7 September 2019. Bari (Italy).

[8] M. Santamouris, Using cool pavements as a mitigation strategy to fight urban heat island: a review of the actual developments, Renew. Sustain. Energy Rev. 26 (2013) 224–240, https://doi.org/10.1016/j.rser.2013.05.047.

[9] H. Akbari, C. Cartalis, D. Kolokotsa, A. Muscio, A.L. Pisello, F. Rossi, M. Santamouris, A. Synnefa, N.H. Wong, M. Zinzi, Local climate change and urban heat island mitigation techniques – the state of the art, J. Civ. Eng. Manag. 22 (2016) 1–16, https://doi.org/10.3846/13923730.2015.1111934.

[10] F. Rossi, B. Castellani, A. Presciutti, E. Morini, M. Filipponi, A. Nicolini, M. Santamouris, Retroreflective façades for urban heat island mitigation: experimental investigation and energy evaluations, Appl. Energy 145 (2015) 8–20, https://doi.org/10.1016/j.apenergy.2015.01.129.

[11] V. Costanzo, G. Evola, L. Marletta, in: Urban Heat Stress and Mitigation Solutions: an Engineering Perspective, first ed., Routledge, 2021 https://doi.org/10.1201/9781003045922.

[12] A.M. Gambelli, M. Cardinali, M. Filipponi, A. Nicolini, F. Ross, A normalization procedure to compare retro- reflective and traditional diffusive materials in terms of UHI mitigation potential, AIP Conf. Proc. 2191 (2019), 020085, https://doi.org/10.1063/1.5138818.

[13] M. Cardinali, A. Di Giuseppe, A.M. Gambelli, M. Filipponi, B. Castellani, A. Nicolini, F. Rossi, Glass beads retro-reflective coating for building application: albedo assessment in urban canyon configurations, J. Phys. Conf. 2177 (2022), 012033, https://doi.org/10.1088/1742-6596/2177/1/012033.

[14] E. Morini, B. Castellani, A. Presciutti, E. Anderini, M. Filipponi, A. Nicolini, F. Rossi, Experimental analysis of the effect of geometry and façade materials on urban district's equivalent albedo, Sustainability 9 (2017) 1245, https://doi.org/10.3390/su9071245.

[15] F. Rossi, E. Morini, B. Castellani, A. Nicolini, E. Bonamente, E. Anderini, F. Cotana, Beneficial effects of retroreflective materials in urban canyons: results from seasonal monitoring campaign, J. Phys. Conf. 655 (2015), 012012, https://doi.org/10.1088/1742-6596/655/1/012012.

[16] N. Riedel-Lyngskær, P.B. Poulsen, M.L. Jakobsen, P. Nørgaard, J. Vedde, Value of bifacial photovoltaics used with highly reflective ground materials on single-axis trackers and fixed-tilt systems: a Danish case study, IET Renew. Power Gener. 14 (2020) 3946–3953, https://doi.org/10.1049/iet-rpg.2020.0580.

[17] M.T. Bembe, S.P. Daniel Chowdhury, N. Meeding, E.G. Lekhuleni, M.B. Ayanna, S. Simelane, Effects of Grass and Concrete Reflective Surface on the Performance of Dual Axis Bifacial Solar PV Systems, IEEE PES/IAS PowerAfrica, 2018, pp. 734–738, https://doi.org/10.1109/PowerAfrica.2018.8521143.

[18] S. Sciara, S.J. Suk, G. Ford, Characterizing electrical output of bifacial photovoltaic modules by altering reflective materials, J. Build. Construct. Plann. Res. 4 (2016) 41–55, https://doi.org/10.4236/jbcpr.2016.41003.

[19] A. Di Giuseppe, M. Cardinali, B. Castellani, M. Filipponi, A.M. Gambelli, L. Postrioti, A. Nicolini, F. Rossi, The effect of the substrate on the optic performance of retro-reflective coatings: an in-lab investigation, Energies 14 (2021) 2921, https://doi.org/10.3390/en14102921.

[20] M. Cardinali, A. Di Giuseppe, B. Castellani, M. Filipponi, A. Nicolini, F. Rossi, An investigation towards the optimum design of retro-reflective materials as building envelopes for the enhancement of optical performance, Construct. Build. Mater. 358 (2022), 129466, https://doi.org/10.1016/j.conbuildmat.2022.129466.

[21] Website, Prochima S.r.l, in: https://www.prochima.it/perla-microsfere-di-vetro/. (Accessed 20 December 2022).

[22] Website, INDEX construction systems and Products S.p.A. https://prodottiesoluzioni.indexspa.it/en/. (Accessed 20 December 2022).

[23] F.E. Nicodemus, Reflectance nomenclature and directional reflectance and emissivity, Appl. Opt. 9 (1970) 1474–1475, https://doi.org/10.1364/AO.9.001474.